10-1-1996

Infrared quarter-wave reflection retarders designed with high-spatial-frequency dielectric surface-relief gratings on a gold substrate at oblique incidence

Jian Liu

Rasheed M.A. Azzam

University of New Orleans, razzam@uno.edu

Infrared quarter-wave reflection retarders designed with high-spatial-frequency dielectric surface-relief gratings on a gold substrate at oblique incidence

Jian Liu and R. M. A. Azzam

One- and two-dimensional high-spatial-frequency dielectric surface-relief gratings on a Au substrate are used to design a high-reflectance quarter-wave retarder at 70° angle of incidence and 10.6-μm light wavelength. The equivalent homogeneous anisotropic layer model is used. It is shown that equal and high reflectances (>98.5%) for the *p* and the *s* polarizations and quarter-wave retardation can be achieved with two-dimensional ZnS surface-relief gratings. Sensitivities to changes of incidence angle, light wavelength, grating filling factor, and grating layer thickness are considered. © 1996 Optical Society of America

1. Introduction

External-reflection phase retarders with high reflectance have been of interest for many years.[1–7] By the selection of the angle of incidence, film thickness, and refractive indices of both the film and metallic substrate, the *p*- and *s*-polarized components of incident monochromatic light can be reflected equally and with a specified differential reflection phase shift introduced between them. In general, these studies involved isotropic films. Azzam and Perilloux[1] discussed the constraint on the optical constants of a film–substrate system such that it functions as a quarter-wave retarder (QWR) or half-wave retarder (HWR) at incidence angles of 70° and 45°, respectively. The restrictions on film and substrate materials limit the design of QWR's and HWR's to the near-UV–visible–near-IR spectral region. Howlader and Azzam[2] have recently proposed a QWR design with very high reflectance at a 45° incidence angle by using periodic and quasi-periodic non-quarter-wave multilayer coatings at 3.39-μm wavelength.

In the IR spectral range, external-reflection optical elements are even more important. However, it is difficult to make an ideal coated QWR or HWR because of the limitation in selecting materials. In recent years binary optics technology and high-resolution lithography have been introduced to fabricate high-spatial-frequency dielectric surface-relief gratings, whose properties are equivalent to those of a thin film if the grating period is small enough to cut off all nonzero diffracted orders. The most important advantage of such subwavelength-structured surfaces is that the needed index can be obtained by a change in the filling factor and the grating period.[8–13] This property overcomes the problem of selecting a material with a proper refractive index in the IR spectral region. High-spatial-frequency gratings have been used for antireflection designs.[9–15]

Both one-dimensional (1-D) and two-dimensional (2-D) dielectric surface-relief gratings exhibit form birefringence. The theory of 1-D dielectric surface-relief gratings has been reviewed by Brundrett *et al.*[11] The 2-D dielectric gratings are described by Grann *et al.*[13] and Motamedi *et al.*[14]

In this paper, the equivalent homogeneous anisotropic layer model (EHALM) is used to analyze how the filling factor and the grating region thickness control the reflected light polarization for 1-D and 2-D dielectric surface-relief gratings on a metallic substrate. This demonstrates the potential of employing such surface-relief gratings to realize a QWR with high reflectance. We select the CO_2 laser wave-

The authors are with the Department of Electrical Engineering, University of New Orleans, New Orleans, Louisiana 70148.

Received 13 November 1995; revised manuscript received 20 February 1996.

0003-6935/96/285557-06$10.00/0

length of 10.6 μm and an incidence angle of 70° as an example.

Section 2 presents the reflection properties of a homogeneous uniaxial film on a metallic substrate. The EHALM is introduced in Section 3. Section 4 illustrates the best QWR design that we obtain by using a 2-D ZnS high-spatial-frequency surface-relief grating on a Au substrate. A comparison with homogeneous isotropic coatings on Au is also discussed in this section. Finally, Section 5 summarizes the paper.

2. Reflection Coefficients for a Homogeneous Uniaxial Film on a Metallic Substrate

Consider an ambient–film–substrate (or three-phase) system, in which the film is uniaxial with the optic axis perpendicular to the interfaces. Because of symmetry, an incident wave in the ambient, which is either p or s polarized, excites waves in the uniaxial film and in the isotropic substrate that possess the same polarization, i.e., p or s, respectively. The complex reflection coefficients are given by[16,17]

$$R\gamma = [r_{12\gamma} + r_{23\gamma}\exp(-j2\beta_\gamma)]/[1 + r_{12\gamma}r_{23\gamma}\exp(-j2\beta_\gamma)], \quad \gamma = pp, ss, \tag{1}$$

where r_{12pp}, r_{23pp} and r_{12ss}, r_{23ss} are the complex amplitude reflection coefficients at the 1–2 (ambient–film) and 2–3 (film–substrate) interfaces for the p and the s polarizations, respectively. They are obtained by

$$r_{12pp} = (N_oN_e\cos\phi_1 - n_1p_1)/(N_oN_e\cos\phi_1 + n_1p_1), \tag{2}$$

$$r_{23pp} = (-N_oN_e\cos\phi_3 + n_3p_3)/(N_oN_e\cos\phi_3 + n_3p_3), \tag{3}$$

$$r_{12ss} = (n_1\cos\phi_1 - s_1)/(n_1\cos\phi_1 + s_1), \tag{4}$$

$$r_{23ss} = (-n_3\cos\phi_3 + s_3)/(n_3\cos\phi_3 + s_3), \tag{5}$$

where

$$p_1 = (N_e^2 - n_1^2\sin^2\phi_1)^{1/2}, \tag{6}$$

$$p_3 = (N_e^2 - n_3^2\sin^2\phi_3)^{1/2}, \tag{7}$$

$$s_1 = (N_o^2 - n_1^2\sin^2\phi_1)^{1/2}, \tag{8}$$

$$s_3 = (N_o^2 - n_3^2\sin^2\phi_3)^{1/2}. \tag{9}$$

The phase thicknesses β_{pp} and β_{ss} of the layer for the p and the s polarizations that appear in Eq. (1) are given by

$$\beta_{pp} = (2\pi\, d/\lambda)(N_o/N_e)p_1, \tag{10}$$

$$\beta_{ss} = (2\pi\, d/\lambda)s_1, \tag{11}$$

where d is the layer thickness, λ is the incident-light wavelength, n_1 is the refractive index of the isotropic ambient, ϕ_1 is the angle of incidence, ϕ_3 is the angle of refraction in the metal substrate with complex refractive index n_3, and N_o and N_e are the ordinary and the extraordinary refractive indices of the uniaxial film, respectively.

When the optic axis of the film is parallel to the interfaces and to the plane of incidence, the corresponding reflection coefficients and phase thicknesses pertaining to Eq. (1) are[18,19]

$$r_{12pp} = (N_oN_e\cos\phi_1 - n_1s_1)/(N_oN_e\cos\phi_1 + n_1s_1), \tag{12}$$

$$r_{23pp} = (-N_oN_e\cos\phi_3 + n_3s_3)/(N_oN_e\cos\phi_3 + n_3s_3), \tag{13}$$

$$r_{12ss} = (n_1\cos\phi_1 - s_1)/(n_1\cos\phi_1 + s_1), \tag{14}$$

$$r_{23ss} = (-n_3\cos\phi_3 + s_3)/(n_3\cos\phi_3 + s_3); \tag{15}$$

$$\beta_{pp} = (2\pi\, d/\lambda)(N_e/N_o)s_1, \tag{16}$$

$$\beta_{ss} = (2\pi\, d/\lambda)s_1. \tag{17}$$

If the film's optic axis is parallel to the interfaces and perpendicular to the plane of incidence, we have

$$r_{12pp} = (N_o^2\cos\phi_1 - n_1s_1)/(N_o^2\cos\phi_1 + n_1s_1), \tag{18}$$

$$r_{23pp} = (-N_o^2\cos\phi_3 + n_3s_3)/(N_o^2\cos\phi_3 + n_3s_3), \tag{19}$$

$$r_{12ss} = (n_1\cos\phi_1 - p_1)/(n_1\cos\phi_1 + p_1), \tag{20}$$

$$r_{23ss} = (-n_3\cos\phi_3 + p_3)/(n_3\cos\phi_3 + p_3); \tag{21}$$

$$\beta_{pp} = (2d\pi/\lambda)s_1, \tag{22}$$

$$\beta_{ss} = (2d\pi/\lambda)p_1. \tag{23}$$

The reflection coefficients and phase thicknesses for a homogeneous anisotropic film on a metallic substrate are obviously more complicated than those for a homogeneous isotropic film. However, there are more degrees of freedom to adjust in designing an external-reflection QWR.

As conical diffraction is not considered in this paper, the subscripts pp or ss are replaced below by p or s, respectively.

The intensity (or power) reflectance is given by

$$\mathcal{R}_\gamma = |R_\gamma|^2. \tag{24}$$

For an external-reflection QWR, the ratio of complex reflection coefficients for the p and the s polarizations must satisfy the condition

$$\rho = R_p/R_s = |R_p/R_s|\exp(j\Delta) = \pm j, \tag{25}$$

in which Δ is the differential reflection phase shift. QWR is achieved if and only if the p- and the s-polarized components are reflected equally and their differential phase shift is ±90°.

3. Equivalent Homogeneous Anisotropic Layer Model for One-Dimensional and Two-Dimensional Dielectric Surface-Relief Gratings

Figure 1 shows a 1-D rectangular-groove grating region, which is situated on a metallic substrate with complex refractive index n_3 and in an ambient with refractive index $n_1 = 1.0$. The grating is etched in a dielectric coating material with refractive index n_c.

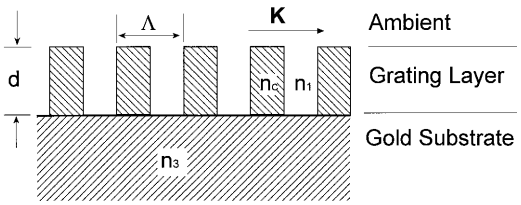

Fig. 1. Cross section of a 1-D dielectric surface-relief grating on a Au substrate.

The grating region thickness is d, the period is Λ, the filling factor is f, and the grating vector is **K**. If the wavelength-to-period ratio (λ/Λ) is large enough to cut off all nonzero diffracted orders, we may use the EHALM.[11] In this model the grating region is described by a slab of uniaxial material with its optic axis parallel to the grating vector. The equivalent ordinary and extraordinary indices of the slab depend on the grating filling factor, the refractive indices of the ambient and the coating material, and the ratio of wavelength to grating period λ/Λ. Also, for $\lambda/\Lambda > \sim 15$, Brundrett *et al.*[11] indicated that higher-order indices are essentially the same as the first-order indices. In this paper, the assumed light wavelength is 10.6 μm, for which large ratios λ/Λ are practical and justify the use of the equivalent first-order indices to analyze the reflection properties of the high-spatial-frequency surface-relief gratings.

The equivalent first-order ordinary and extraordinary refractive indices are determined by[11]

$$N_o = (1 - f + n_c^2 f)^{1/2}. \tag{26}$$

$$N_e = (1 - f + f/n_c^2)^{-1/2}. \tag{27}$$

Figure 2 shows a 2-D periodic dielectric surface-relief square-pillar grating, with volume filling factor f, thickness d, and refractive index n_c for the coating material. The substrate is a metal with complex refractive index n_3. The period Λ of the grating along each side of the square is much smaller than the incident-light wavelength λ, so that $\lambda/\Lambda > 15$ in each direction.

Similar to the 1-D dielectric surface-relief grating, the 2-D square-pillar grating can also be treated with the EHALM. The optic axis for the 2-D square-pillar grating is parallel to the pillars and normal to the interfaces of the EHALM. The effective ordinary index is obtained by assuming a 50%–50% dielectric mixture of the values given in Eqs. (26) and (27). By the squaring and averaging of Eqs. (26) and (27), the effective ordinary refractive index is obtained[14]:

$$N_o = (\{(1 - f + f n_c^2)[f + (1 - f) n_c^2] + n_c^2\}/\{2[f + (1 - f) n_c^2]\})^{1/2}, \tag{28}$$

where the volume filling factor $f = (a/\Lambda)^2$ and a is the width of the square pillar for a 2-D surface-relief grating.

The effective principal extraordinary index has the form[12,13]

$$N_e = (1 - f + f n_c^2)^{1/2}. \tag{29}$$

Therefore the 2-D dielectric surface-relief grating with square pillars is equivalent to a uniaxially anisotropic layer with the optic axis parallel to the pillars and with effective ordinary and extraordinary indices N_o and N_e that vary with the volume filling factor.

The EHALM is used for the analysis of the reflected polarization states and for the design of the QWR by the use of high-spatial-frequency dielectric surface-relief gratings.

4. Quarter-Wave Retarder Design with a Two-Dimensional High-Spatial Frequency ZnS Surface-Relief Grating on a Au Substrate

Figure 3 shows the differential reflection phase shift Δ versus angle of incidence for a bare Au substrate with refractive index of $n_3 = 12.67 - j71.40$ at $\lambda = 10.6$ μm.[20] The principal angle at which a 90° differential phase shift is achieved is 89.21°; the associated unequal intensity reflectances are $\mathcal{R}_p = 70.25\%$ and $\mathcal{R}_s = 99.99\%$. Even though Au is a good material to use in the IR spectral region for making high-reflectance mirrors, the high slope at the principal angle of $\delta\Delta/\delta\phi \simeq 74$ deg/deg, the large difference

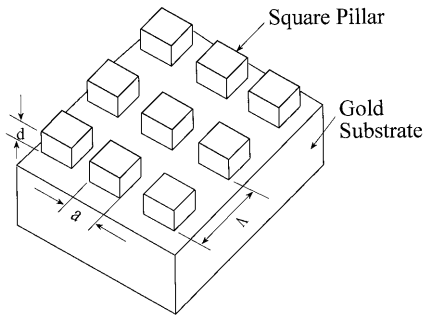

Fig. 2. Geometry of a 2-D dielectric surface-relief grating with square pillars.

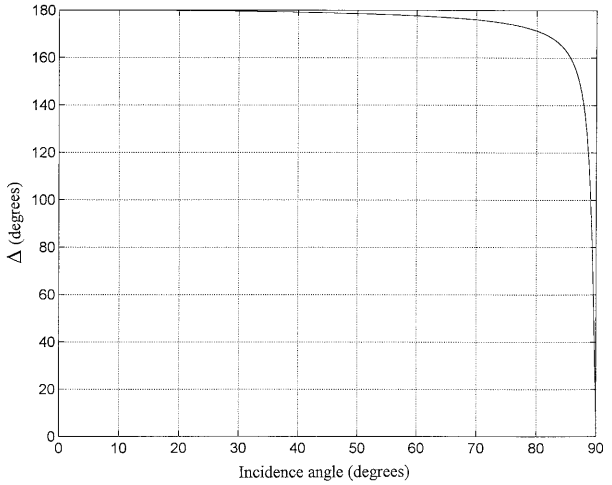

Fig. 3. Differential reflection phase shift Δ versus angle of incidence for a bare Au substrate at light wavelength $\lambda = 10.6$ μm.

Table 1. Five Selected QWR's at 70° Incidence Angle and 10.6-μm Light Wavelength Designed with a Homogeneous Isotropic Film on a Au Substrate

Number	n_2	d (μm)	$\mathcal{R}_p$ (%)	$\mathcal{R}_s$ (%)	$\mathcal{R}_{av}$	$\mathcal{R}_p/\mathcal{R}_s$	$\Delta + 360$
1	1.8100	1.05625	99.0699	98.1147	98.5923	1.0097	90.0006
2	2.0100	0.8875	98.9440	98.2058	98.5749	1.0075	89.9935
3	2.2175	0.79125	98.8239	98.1107	98.4673	1.0073	89.9936
4	2.3975	0.7325	98.7165	97.9755	98.3460	1.0076	90.0033
5	2.6725	0.66675	98.5410	97.6978	98.1194	1.0086	89.9612

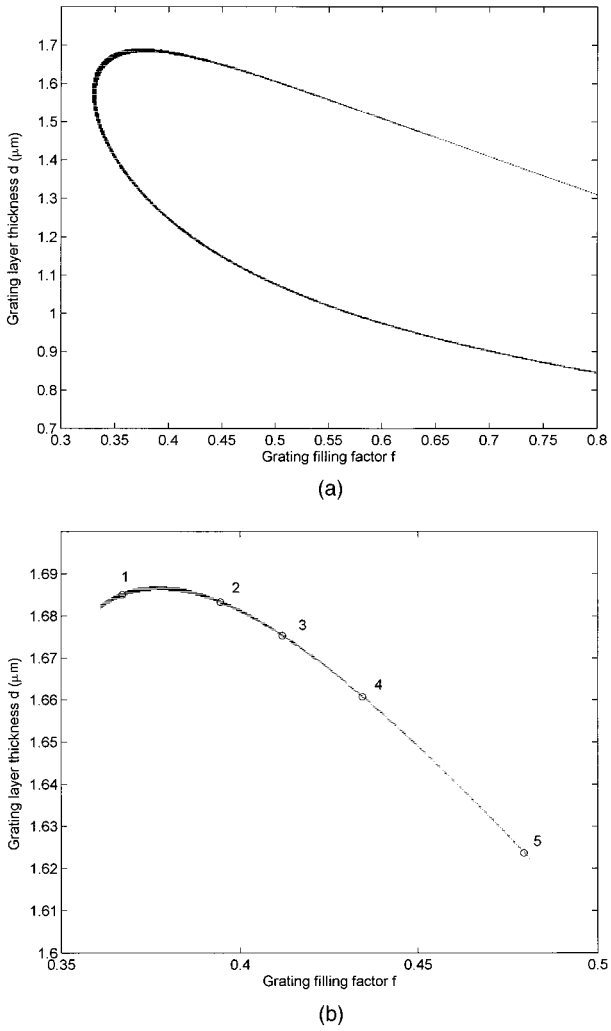

Fig. 4. Locus of grating region thickness d versus grating filling factor f for QWR designs with (a) $|\rho| = 1.00 \pm 0.01$ and $|\Delta| = 90° \pm 0.1°$, (b) $|\rho| = 1.000 \pm 0.001$ and $|\Delta| = 90° \pm 0.01°$.

between the p and the s reflectances and the near-grazing incidence angle make it impractical as a QWR.

When a uniform homogeneous isotropic film is deposited on the Au substrate, the reflection properties of the Au can be modified to obtain a QWR.[1] Table 1 shows five selected QWR designs at an incidence angle of 70° and a light wavelength of 10.6 μm. The main disadvantage of using an isotropic coating on a Au substrate is the difficulty in finding

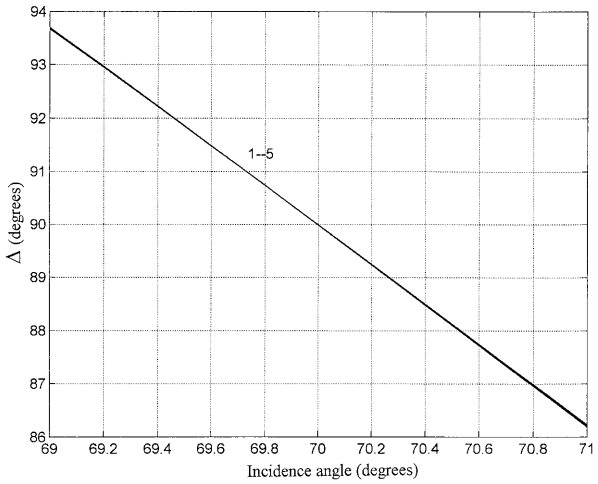

Fig. 5. Differential reflection phase shift Δ as a function of incidence angle for the five QWR designs listed in Table 2.

the required coating materials. Also, the intensity reflectances cannot reach very high values for all designs.

We have designed 1-D and 2-D high-spatial-frequency surface-relief gratings on a Au substrate that function as QWR's at the 70° angle of incidence by using several readily available dielectric materials including ZnS and Si, which have refractive indices 2.2176 and 3.4215, respectively, at $\lambda = 10.6$ μm.[21] We find that the 2-D ZnS square-pillar surface-relief grating on Au offers the best results.

Figure 4(a) shows the locus of all possible solutions (f, d) that achieve QWR with $|\rho| = 1.00 \pm 0.01$ and $|\Delta| = 90° \pm 0.1°$. As the accuracies are raised to $|\rho| = 1.000 \pm 0.001$ and $|\Delta| = 90° \pm 0.01°$, only the upper left part of the curve, shown in Fig. 4(b), is obtained. Five designs, represented by points 1, 2, 3, 4, and 5, are selected for sensitivity analysis (see Table 2).

Figure 5 illustrates that the angular sensitivity of the differential phase shift is nearly the same for all five designs. A 1° angle-of-incidence error causes $<3.8°$ error for the differential phase shift for the five designs. Figure 6 shows the intensity reflectance ratio versus incidence angle. Over the entire region of incidence angle, the deviation of the reflectance ratio from 1.000 is within ± 0.0023. The average reflectance versus incidence angle is drawn in Fig. 7 and is $>98.5\%$ between 69° and 71°. Figure 8 demonstrates the sensitivity to changes of the incident-light wavelength λ from 10.0 to 11.2 μm. The

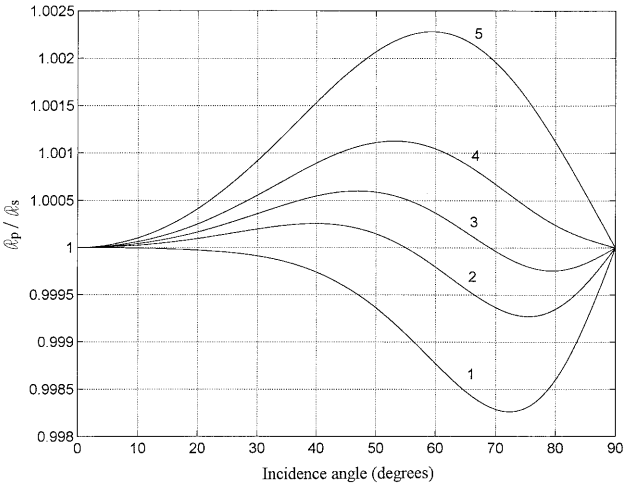

Fig. 6. Intensity reflectance ratio as a function of incidence angle for the five QWR designs listed in Table 2.

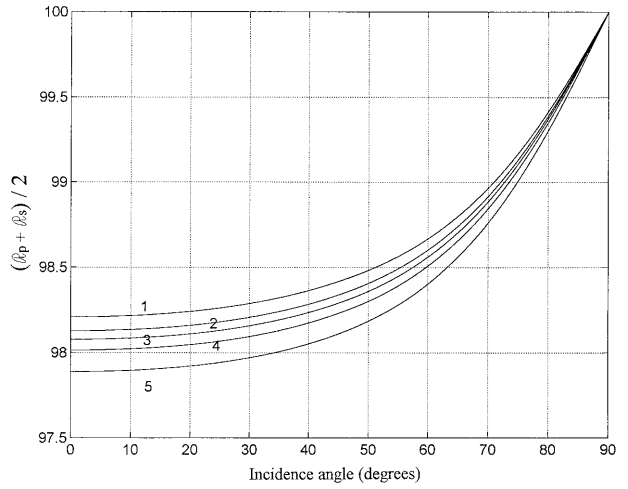

Fig. 7. Average reflectance as a function of incidence angle for the five QWR designs listed in Table 2.

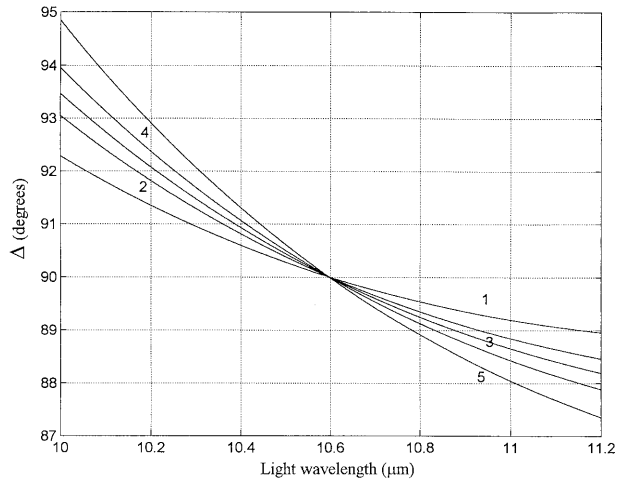

Fig. 8. Differential reflection phase shift Δ as a function of the incident-light wavelength λ for the five QWR designs listed in Table 2.

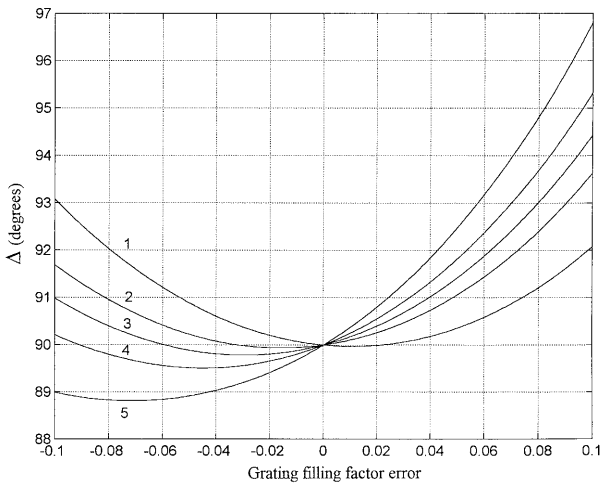

Fig. 9. Sensitivity of the differential reflection phase shift Δ to error of the grating filling factor f for the five QWR designs listed in Table 2.

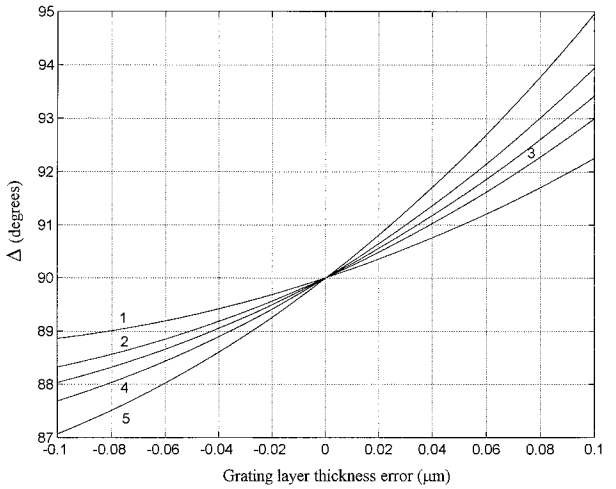

Fig. 10. Sensitivity of the differential reflection phase shift Δ to error of the grating-region thickness d for the five QWR designs listed in Table 2.

corresponding sensitivities to changes of the grating filling factor (by ± 0.1) and grating-region thickness (by ± 0.1 μm) appear in Figs. 9 and 10, respectively. The average reflectance and the reflectance ratio of these designs are not significantly sensitive to changes of light wavelength, grating filling factor, or grating-region thickness. Average reflectances remain $>98.5\%$ and the reflectance ratios differ from 1 by $<0.5\%$.

If we consider that the differential reflection phase shift is the most important parameter for a QWR, design 1 in Table 2 can be regarded as the best one. For this design the maximum phase error is $\sim 2.3°$ for a 0.6-μm incident-light wavelength shift, 3.1° for a 0.1 filling factor error, and 2.25° for a 0.1-μm thickness error. The average reflectance is 98.9638%.

Table 2. Five QWR's at 70° Incidence Angle and 10.6-μm Light Wavelength Designed with a 2-D ZnS Grating on a Au Substrate

Number	f	d (μm)	$\mathcal{R}_p$ (%)	$\mathcal{R}_s$ (%)	$\mathcal{R}_{av}$	$\mathcal{R}_p/\mathcal{R}_s$	$\Delta + 360^o$
1	0.3670	1.6850	98.8790	99.0486	98.9638	0.9983	89.9997
2	0.3945	1.6833	98.8839	98.9465	98.9152	0.9994	89.9993
3	0.4120	1.6753	98.8822	98.8857	98.8840	1.0000	89.9991
4	0.4345	1.6607	98.8764	98.8102	98.8433	1.0007	89.9954
5	0.4795	1.6237	98.8564	98.6633	98.7599	1.0020	89.9904

5. Summary

We have demonstrated that a 2-D high-spatial-frequency surface-relief grating etched in a ZnS coating that is deposited on a Au substrate offers a QWR with equal and high p and s reflectances (>98.5%) at an incidence angle of 70° and a light wavelength of 10.6 μm. This external-reflection QWR is reasonably insensitive to changes of the incident-light wavelength, grating-region filling factor and thickness, and incidence angle.

This research was supported by the U.S. National Science Foundation and presented at the Annual Meeting of the Optical Society of America in Portland, Or., 10–15 September 1995.

References

1. R. M. A. Azzam and B. E. Perilloux, "Constraint on the optical constants of a film–substrate system for operation as an external-reflection retarder at a given angle of incidence," Appl. Opt. **24,** 1171–1179 (1985).
2. M. M. K. Howlader and R. M. A. Azzam, "Periodic and quasi-periodic nonquarterwave multilayer coatings for 90-deg reflection phase retardance at 45-deg angle of incidence," Opt. Eng. **34,** 869–874 (1995).
3. W. H. Southwell, "Multilayer coating design achieving a broadband 90° phase shift," Appl. Opt. **19,** 2688–2692 (1980).
4. J. H. Apfel, "Phase retardance of periodic multilayer mirrors," Appl. Opt. **21,** 733–738 (1982).
5. R. M. A. Azzam and M. E. R. Khan, "Single-reflection film–substrate half-wave retarders with nearly stationary reflection properties over a wide range of incidence angles," J. Opt. Soc. Am. **73,** 160–166 (1983).
6. A. Röseler, *Infrared Spectroscopic Ellipsometry* (Akademie-Verlag, Berlin, 1990).
7. R. M. A. Azzam, A.-R. M. Zaghloul, and N. M. Bashara, "Ellipsometric function of a film–substrate system: applications to the design of reflection-type optical devices and to ellipsometry," J. Opt. Soc. Am. **65,** 252–260 (1975).
8. R. C. Enger and S. K. Case, "Optical elements with ultrahigh spatial-frequency surface corrugation," Appl. Opt. **22,** 3220–3228 (1983).
9. K. Gaylord, E. N. Glytsis, and M. G. Moharam, "Zero-reflectivity homogeneous layers and high spatial-frequency surface-relief gratings on lossy materials," Appl. Opt. **26,** 3123–3135 (1987).
10. K. Gaylord, E. N. Glytsis, M. G. Moharam, and W. E. Baird, "Technique for producing antireflection grating surfaces on dielectrics, semiconductors, and metals," U.S. Patent 5,007,708 (16 April 1991).
11. D. L. Brundrett, E. N. Glytsis, and T. K. Gaylord, "Homogeneous-layer models for high-spatial-frequency dielectric surface-relief gratings: conical diffraction and antireflection designs," Appl. Opt. **33,** 2695–2706 (1994).
12. D. C. Flanders, "Submicrometer-periodicity gratings as artificial dielectrics," Appl. Phys. Lett. **42,** 492–494 (1983).
13. E. B. Grann, M. G. Moharam, and D. A. Pommet, "Artificial uniaxial and biaxial dielectrics with use of two-dimensional subwavelength binary gratings," J. Opt. Soc. Am. A **11,** 2695–2703 (1994).
14. M. E. Motamedi, W. H. Southwell, and W. J. Gunning, "Antireflection surfaces in silicon using binary optics technology," Appl. Opt. **31,** 4371–4376 (1992).
15. A. M. Kan'an and R. M. A. Azzam, "In-line quarter-wave retarders for the infrared using total refraction and total internal reflection in a prism," Opt. Eng. **33,** 2029–2033 (1994).
16. A. Yariv and P. Yeh, *Optical Waves in Crystals* (Wiley, New York, 1984).
17. D. D. Engelsen, "Ellipsometry of anisotropic films," J. Opt. Soc. Am. **61,** 1460–1466 (1971).
18. J. Lekner, "Reflection and refraction by uniaxial crystals," J. Phys.: Condens. Matter **3,** 6121–6133 (1991).
19. R. M. A. Azzam and N. M. Bashara, *Ellipsometry and Polarized Light* (North-Holland, Amsterdam, 1977).
20. M. A. Ordal, L. L. Long, R. J. Bell, S. E. Bell, R. R. Bell, R. W. Alexander Jr., and C. A. Ward, "Optical properties of the metals Al, Co, Cu, Au, Fe, Pb, Ni, Pd, Pt, Ag, Ti, and W in the infrared and far infrared," Appl. Opt. **22,** 1099–1119 (1983).
21. E. D. Palik, ed., *Handbook of Optical Constants of Solids* (Academic, New York, 1985).